

## The frequency characteristics of anomalous vertical fields observed in the British Isles

**D. Beamish**

British Geological Survey, Murchison House, West Mains Road, Edinburgh EH9 3LA, United Kingdom

**Abstract.** The frequency characteristics of anomalous vertical fields are presented and summarised in a consistent manner across a substantial area of the UK. The period range considered is from 10 to 10000 s. The results have been necessarily divided into coastal and non-coastal observations. An effective coast-effect has been observed at only one location, on the west coast of Ireland. At other coastal sites, individual frequency characteristics are observed that appear dependent on site location. The controlling regional influence of the deep ocean and shelf seas at periods in excess of 1000 s is noted and to some extent defined in the results obtained across a major portion of the UK land-mass.

When mainland results are compared on a regional basis, spatially consistent features emerge in both the real and imaginary induction arrows. The results demonstrate that the in-quadrature component of the anomalous vertical field, although often small (i.e.  $<0.1$ ), can be determined with sufficient accuracy to provide information as characteristic and detailed as that of the in-phase component. When transfer function estimates are well-resolved, it is demonstrated that the frequency characteristics observed in the azimuth differences and phase of the anomalous vertical field can be used to characterise the response observed at a given location. In particular, the detailed behaviour of such parameters with frequency may indicate the degree of near-field 2-dimensionality. A characteristic period, predicted by simple 2-dimensional models, is clearly observed at a number of locations. It is pointed out that such a period is diagnostic of the structural parameters defining the geoelectric anomaly.

**Key words:** Electromagnetic induction – Anomalous vertical fields – Induction arrows – Frequency characteristics – British Isles – Observations – Models

---

### Introduction

Estimates of the anomalous vertical field obtained from geomagnetic sounding experiments contain unique information on lateral contrasts in geoelectric structure. Such transfer function estimates are obtained as a function of frequency across a given bandwidth. The estimates then define frequency response curves at one or more locations. Over the past 15 years several geomagnetic deep sounding experiments conducted in the British Isles have been de-

scribed (Edwards et al., 1971; Hutton and Jones, 1980; Sik et al., 1981; Beamish and Banks, 1983). Across the same time interval data logging and analysis techniques have improved. Over the past 10 years the British Geological Survey has operated digitally recording rubidium and fluxgate magnetometers at a number of locations, in relation to a variety of field experiments. These data have been subjected to a common formatting and analysis technique that provides well-resolved transfer function estimates over the period range 10–10000 s. The results obtained define a set of characteristic frequency response curves from widely dispersed locations across Britain. The aim of this study is to summarise, present and comment on these results. It is hoped that the results presented will form a background to which further observations may be both compared and understood.

The spatially extensive data set considered by Edwards et al. (1971) covered the period range from 720–28800 s. The results obtained were interpreted on the basis of the regional influence exerted by the induced current systems in the ocean and shelf seas. Based mainly on results covering the period range from 2400–8640 s, the authors defined the six major current concentrations shown in Fig. 1, referred to as L1–L6. L1 was defined along the continental slope to the west of Ireland, current concentrations L2–L5 were located in loops within the shelf seas, while L6 defined a current concentration within the Southern Uplands of Scotland. Frequency-dependent effects were noted, particularly at sites in Ireland, as the period decreased and the relative strength of the current systems in the shelf seas increased. These long-period frequency characteristics were also observed in the analogue model study of the British Isles presented by Dosso et al. (1980). The authors considered scale model results equivalent to the period range 1200–7200 s and the results indicate that over this interval the anomalous vertical field may change by a factor of five or six between certain coastal locations, and at least by a factor of two or three between inland locations.

In the geomagnetic array study of Scotland (Sik et al., 1981; Kirkwood et al., 1981), transfer function results were presented down to a period of 300 s although no explicit use was made of their frequency characteristics. More recently, Banks and Beamish (1984) used the frequency characteristics observed across a dense network of sites in southern Scotland and northern England to investigate the mechanisms of local and regional induction. At periods greater than 2000 s, the transfer functions at the majority of sites



Fig. 1. Location of six current concentrations (L1–L6) in and around the British Isles, at a period of 2400 s. After Edwards et al. (1971)

are determined by current concentrations associated with the Atlantic ocean to the west and south-west. In the period range 400–2000 s, the transfer functions are determined by currents induced in a thin sheet of laterally varying conductance comprising shallow seas and both on- and off-shore sedimentary basins. At periods less than 200 s, the transfer functions are compatible with an induction process which is controlled by the local geological structure.

In the present study the results are necessarily divided into coastal and non-coastal observations. In each case the frequency response curves obtained are compared with the equivalent results obtained from simple models. General methods for the interpretation of anomalous fields using their frequency characteristics have been considered by Rokityansky (1975, 1982). The existence and properties of a characteristic period generated by simple geoelectric structures may be used to further characterise a frequency response curve. The accuracy and broadband nature of the response curves considered allows such characteristics to be examined in detail.

### Transfer functions and their presentation

The data considered in the present study are single-site vertical-field transfer functions. These relate the vertical and horizontal components of the magnetic variation field as a function of frequency at a particular location. Although certain necessary assumptions must be made concerning single-site data (Schmucker, 1970; Banks, 1973), the transfer functions obtained from such data avoid the requirement for simultaneous operation of instruments and enable a basic response set to be generated using data col-

lected at different times. Such an advantage outweighs the limitations of the approach for the present comparative study. The geomagnetic data for this study were obtained from both fluxgate and rubidium vapour magnetometers, recording digitally on cassettes. The procedures used to determine the single-site transfer function ( $A$ ,  $B$ ) from such data are given by Beamish and Banks (1983). The method used provides band-averaged transfer function estimates over the three decades from 10 to 10000 s. These three decades are divided logarithmically into 18 overlapping period bands.

The magnitude of the transfer functions generally observed in the U.K. is small (e.g.  $\ll 0.5$ ) and we require well-resolved estimates if detailed information is to be obtained. An important aspect of the present study is that the procedure adopted, together with the amount of data analysed, provides well-estimated transfer functions that are smooth functions of frequency. In particular, the phase information contained in the transfer function is accurately determined. The data have been subject to the same analysis procedure with the result that stable and accurate transfer functions can be presented and compared.

The single-site vertical-field transfer function consists of the complex pair of numbers ( $A$ ,  $B$ ) determined as a function of frequency or period band. The most common method of presentation is the induction arrow which allows the transfer function to be presented in terms of a magnitude and an azimuth which defines the normal to the strike of a local geoelectric lateral gradient giving rise to an anomalous concentration of current. Two such arrows are defined for vertical fields responding in-phase (real) and in-quadrature (imaginary) with the horizontal component with which the vertical field possesses maximum correlation. The magnitudes of the real and imaginary induction arrows are defined as

$$G_R = (A_R^2 + B_R^2)^{1/2}$$

$$G_I = (A_I^2 + B_I^2)^{1/2}, \quad (1)$$

where the subscripts  $R$  and  $I$  refer to the real and imaginary parts. The azimuths of the real and imaginary induction arrows are here defined as

$$\theta_R = \tan^{-1} (B_R/A_R)$$

$$\theta_I = \tan^{-1} (B_I/A_I) \quad (2)$$

clockwise from geomagnetic north. It can be noted that both real and imaginary induction arrows are reversed, in keeping with an implied time dependence of  $\exp(i\omega t)$ , (Lilley and Arora, 1982). The induction-arrow method of presentation has a simple interpretation only when the structure is 2-dimensional. In such circumstances, given suitable ratios of conductivity contrast and frequency, the arrows will be perpendicular to the conductivity contrast.

When the transfer function possesses an intermediate phase, the separation into real and imaginary components can be artificial. The maximum and minimum response function presentation of Banks and Ottey (1974) is aimed at separating from ( $A$ ,  $B$ ) that part of the transfer function that is compatible with a 2-dimensional assumption. The presentation again requires four parameters consisting of the maximum and minimum response magnitudes ( $G_M$  and  $G_L$ ), together with the azimuth and phase ( $\theta_M$ ,  $\phi_M$ ) of the maximum response. The three maximum response param-

ters  $G_M$ ,  $\theta_M$ ,  $\phi_M$ , then define that part of the response that is compatible with a 2-dimensional assumption. An example of the eight parameters that can be obtained from the transfer function are shown in Fig. 4, as a function of frequency.

### The frequency response of two simple models

Prior to the presentation and discussion of the observed frequency characteristics, it is worthwhile considering the frequency characteristics that can be derived from simple geoelectric models. When considering the transfer function data set across the U.K. it is necessary to subdivide the site locations into coastal and non-coastal (i.e. mainland) sites. In so doing, it is useful to consider two broad categories of models that have found applications in these two situations. To examine the frequency response that may be observed at coastal sites, a typical thin-sheet geoelectric model is considered. To examine the frequency response that may be observed at mainland sites, a typical 2-dimensional geoelectric model with an embedded anomaly is considered.

The geomagnetic coast effect, reviewed by Parkinson and Jones (1979), is commonly related to the edge, or near, effect produced by electromagnetic induction in an electrically thin, conducting sheet (or shell), taken to represent the ocean. The thin-sheet approximation requires two limiting conditions on the electrical thickness of the surface sheet (Schmucker, 1970, 1971). These conditions impose a lower bound on the variation periods for which the thin-sheet approximation may be used. For the deep (4 km) ocean, the lower period bound lies in the range 900–1000 s (Schmucker, 1971; Weaver, 1979). Solutions to a thin-sheet model can therefore only provide “one-sided” solutions at periods greater than the lower bound.

A number of analytic and numerical procedures have been developed to study the edge-effect of induced currents in thin-sheets (Hewson-Browne and Kendall, 1976; Fischer, 1979). We here consider a solution obtained using a matching technique suggested by Hewson-Browne and Kendall (1976) and applied by Quinney (1979). The model consists of a half-plane of finite conductivity (the ocean) underlain by, and insulated from, a region of perfect conductivity whose upper surface lies at a depth of  $P/2$ .  $P$  is the depth of the image currents induced in the perfect conductor which simulates the conducting Earth. The solutions for the electric field obtained by Quinney (1979) together with the resulting magnetic fields constitute universal curves, being a function of distance  $x$  from the ocean edge, and depend only on the parameter

$$\gamma = 0.5\omega\kappa\mu_0 P, \quad (3)$$

where  $\omega$  is angular frequency,  $\kappa$  is the conductance of the surface half-plane (a constant),  $\mu_0$  is the permeability of free space and  $P$  is defined above.

Solutions to this problem using  $\kappa = 16000$  mho (i.e. for an ocean of depth 4 km) and  $P = 1000$  km have been obtained by D. Quinney for the period range corresponding to the observational bandwidth of the present study. The anomalous vertical field provided by the solution is divided by the total horizontal field to provide a direct comparison with observation. The in-phase and in-quadrature ratios, equivalent to the induction-arrow magnitudes  $G_R$  and  $G_I$ ,

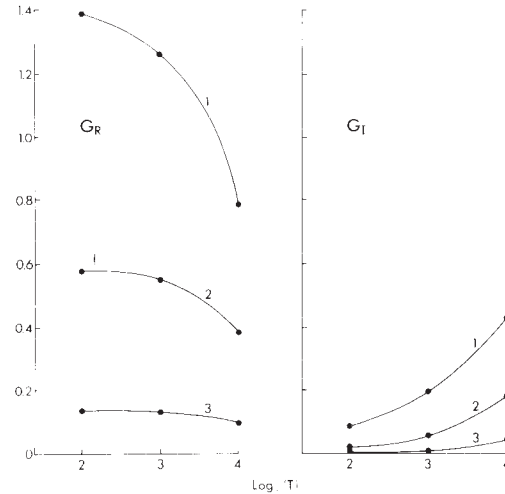


Fig. 2. Induction-arrow magnitudes as a function of period  $T$  (s) and distance ( $x$ ) from the ocean edge, computed from a thin-sheet model.  $G_R$  is real magnitude and  $G_I$  is imaginary magnitude. Curve 1:  $x=0.1$   $P=100$  km. Curve 2:  $x=0.5$   $P=500$  km. Curve 3:  $x=1.0$   $P=1000$  km.

at three locations inland from the ocean edge are shown in Fig. 2. The ratios obtained for (curve 1)  $x=0.1$   $P$  (100 km) can be considered a near-field effect while the ratios obtained for (curve 3)  $x=1.0$   $P$  (1000 km) are a far-field effect of the current concentration at the ocean edge. The frequency characteristics observed for the ratios are similar to the corresponding results obtained for the Roden strip of finite width (Roden, 1964) presented by Edwards et al. (1971, Fig. 23). In the present case, the results have been obtained to much shorter periods. At short periods ( $T < 1000$  s), the solution provides an upper bound in the in-phase response  $G_R$  and a lower bound in the in-quadrature response  $G_I$ . With increasing period ( $T > 1000$  s), a characteristic asymptotic frequency response is observed which is a function of distance from the ocean edge. As noted previously, for a 4-km ocean the results obtained for a thin-sheet model apply for  $T > 900$  s, the equality expressing the likely lower bound for quasi-static induction in the deep ocean. At shorter periods, as  $T \rightarrow 0$ , the induced tangential electric field within the ocean suffers rapid attenuation and the effects of self and mutual induction must be taken into account. The characteristics shown in Fig. 2 reveal that the far-field effect of deep ocean induction may be discernable in  $G_R$  (i.e.  $G_R = 0.1$ ) as far as  $x = 1000$  km.

The solutions provide the constraint that  $G_R > G_I$  over the observational bandwidth. Perhaps the most characteristic feature of the response occurs at the lower bound for quasi-static induction. At this period, the anomalous vertical field will be a maximum and will be predominantly in-phase. An additional feature of the solutions obtained is that the ratios obtained are universal curves depending on the parameter  $\gamma$ . As can be seen from Eq. (3), with  $P$  a constant equivalence is obtained by retaining  $\omega\kappa$  as a constant. We may, in fact, displace all curves one decade lower in period (i.e. to the left) for a sea of depth 0.4 km and the same conductivity. Such curves therefore allow a general assessment of the frequency characteristics of anomalous vertical fields in both the near- and far-fields. The results provided are inevitably one-sided and can only be used to obtain the asymptotic frequency response from a



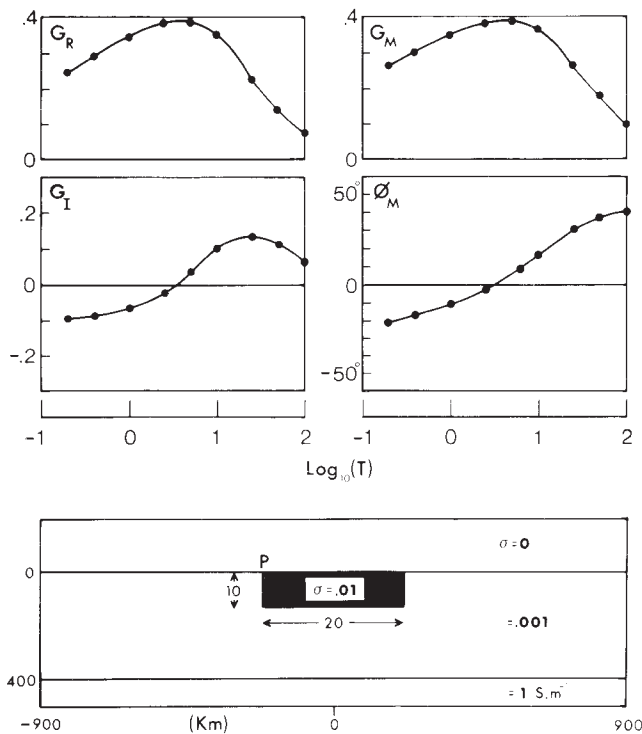


Fig. 3. Two-dimensional model of conducting anomaly (*lower diagram*). Upper four diagrams are frequency response curves of the anomalous vertical field computed at point P.  $G_R$ ,  $G_I$  are the amplitudes of the real and imaginary induction arrows.  $G_M$  and  $\phi_M$  are the magnitude and phase of the maximum response (see text)

lower period bound. The parameter specification of the model, however, makes it one of the simplest that can be applied in the study of the frequency dependence of the anomalous vertical field.

The thin-sheet models discussed above have a limited application when considering the frequency response of the lower two decades (10–1000 s) at sites in mainland U.K. To examine broader-band frequency characteristics we consider instead a simple 2-dimensional numerical model. For our present purposes the simplest model consists of an isolated conducting anomaly embedded in a half-space. Reviews of both analytic and numerical solutions to such problems are provided by Jones (1973), Kaufman and Keller (1981) and Rokityansky (1982). The model considered is defined in Fig. 3, solutions being obtained by a form of the finite difference method (e.g. Pascoe and Jones, 1972; Brewitt-Taylor and Weaver, 1976). The frequency dependence of the four parameters  $G_R$ ,  $G_I$ ,  $G_M$  and  $\phi_M$ , evaluated at point P on the surface is shown in Fig. 3.

The main frequency characteristic of the anomalous vertical field derived from such models is a change of sign in the phase of the vertical field at the frequency where the maximum response is observed. This phase change is a general result of both analytic and numerical models (e.g. Rokityansky, 1982). The phase change can be observed in terms of the induction-arrow azimuths or possibly more directly in terms of the phase of the maximum response. For a 2-dimensional structure the real and imaginary induction-arrow azimuths are strictly parallel or antiparallel. Using the transfer function parameters defined previously, two frequency-dependent conditions are imposed on the parameters derived from the vertical-field transfer function. Let

$T_0$  be the period at which the maximum response is observed, then for  $T < T_0$ , the azimuths of the real and imaginary induction arrows are antiparallel (they differ by  $180^\circ$ ) and the phase of the maximum response is negative. For  $T > T_0$ , the azimuths of the real and imaginary induction arrows are parallel and the phase of the maximum response is positive. At  $T_0$  and for a strictly 2-dimensional structure, the phase of the maximum response is zero and the azimuth of either the real or imaginary induction arrow will change by  $180^\circ$  depending on whether the maximum is observed in  $G_R$  or  $G_I$ . Clearly, in assessing the degree of 2-dimensionality, a consideration of the difference  $\theta_R - \theta_I$  should be a useful exercise, while the condition  $\phi_M = 0$  provides a better assessment of  $T_0$ .

### The frequency response at coastal sites

Transfer function results over three decades are available at five coastal sites, four of these sites lie within the British Isles while the fifth site is on Faroe (FA). One of the sites, Valentia (VA), is situated on the west coast of Ireland and was considered by Parkinson (1962) to be a 'normal' coast site in that the vertical field is strongly influenced by the west-European continental shelf. The frequency response of the eight parameters that may be used to characterise the transfer function are shown in Fig. 4, for VA. The upper four curves define the magnitude and azimuth of the two induction arrows while the lower four curves define the maximum and minimum response parameters. It can be noted in Fig. 4 that since the response is largely in-phase, i.e.  $G_R > G_I$ , there is a high degree of equivalence between the upper and lower methods of presentation.

Our purpose here is to summarise the frequency dependence of these parameters at the five widely separated coastal sites shown in Fig. 5 in relation to the bathymetry of the continental margin. The coastal sites are denoted as FA, LE, DU, HA and VA. We first restrict our attention to the estimates obtained from the first five long-period bands of the analysis. These bands cover the period range 7200–900 s. The azimuthal information contained in the transfer function is best considered using  $\theta_M$ , the azimuth of the maximum response considered in isolation from the additional complexities of amplitude and phase. The azimuths obtained for the period range 7200–900 s at the five coastal sites, together with four mainland sites shown for comparison, are displayed in Fig. 5. The sense of rotation with decreasing period is indicated by arrows.

It is quite evident from Fig. 5 that the long-period anomalous vertical fields are strongly influenced by induced current systems within both the deep ocean and shelf seas. Despite the lack of deep ocean between the west Shetland (LE) and Faroe (FA) platforms, a concentration of current exists in the shelf seas (<1 km) separating the two islands. It is also apparent that, while the azimuths at the coastal sites are relatively constrained over the bandwidth considered, the azimuths at three of the inland sites (ES, YO and CA) rotate through a large angle, from the NW to the NE quadrant, with decreasing period. The consistent rotation pattern displayed at the six sites LE, DU, LL, ES, YO and CA is indicative of a large-scale effect extending over a large part of mainland Britain and has been commented upon by Banks and Beamish (1984). At 10000 s the anomalous fields are dominated by the current system in the deep ocean to the west and SW. As the period de-

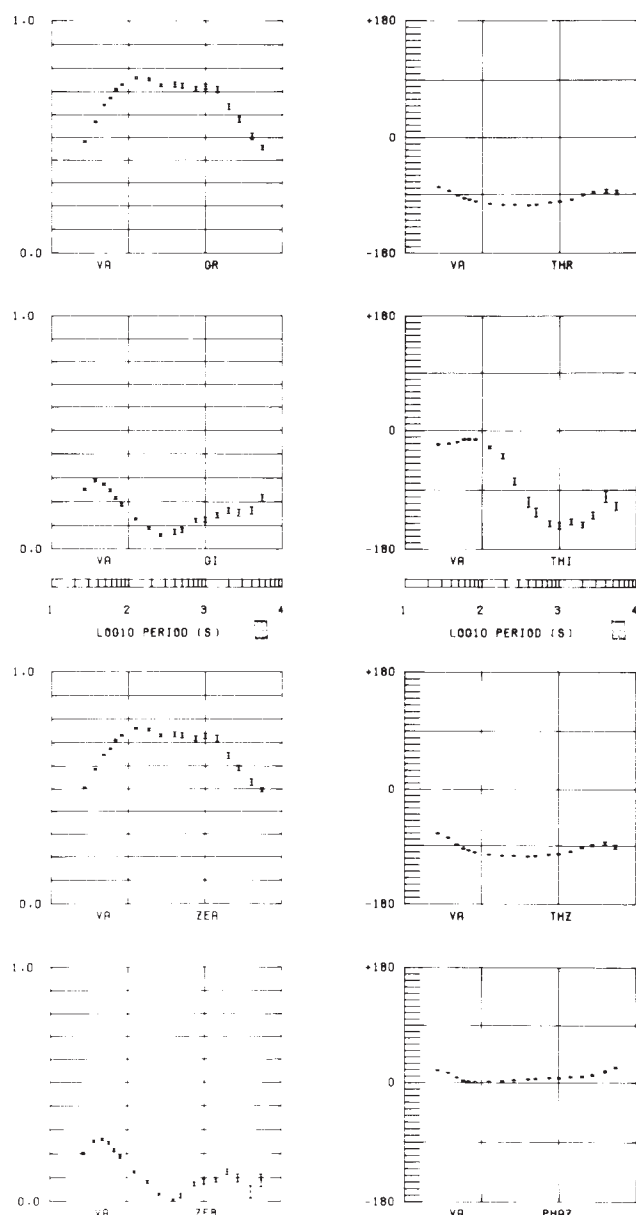


**Fig. 4.** Frequency response of the anomalous vertical field at Valentia VA. Upper four diagrams are induction-arrow parameters.  $G_R$ , THR: magnitude and azimuth of the real induction arrow.  $G_I$ , THI: magnitude and azimuth of the imaginary induction arrow. Lower four diagrams are the maximum/minimum response parameters. ZEA, ZEB: magnitude of the maximum and minimum response. THZ: azimuth of the maximum response. PHAZ: phase of the maximum response

creases, the relative importance of currents to the east in the North Sea increases causing the observed rotations.

We now consider the frequency response observed in the magnitude of the anomalous vertical field at the same five coastal sites. The frequency response is presented in terms of the induction-arrow amplitudes  $G_R$  and  $G_I$ . The results for VA are shown in Fig. 4 and the results for the other four sites are plotted on a common scale in Fig. 6. It is apparent that the frequency response curves observed at each site are highly individual. Before considering their general characteristics we must note from Fig. 5 the complex distribution of offshore bathymetric units which reflect

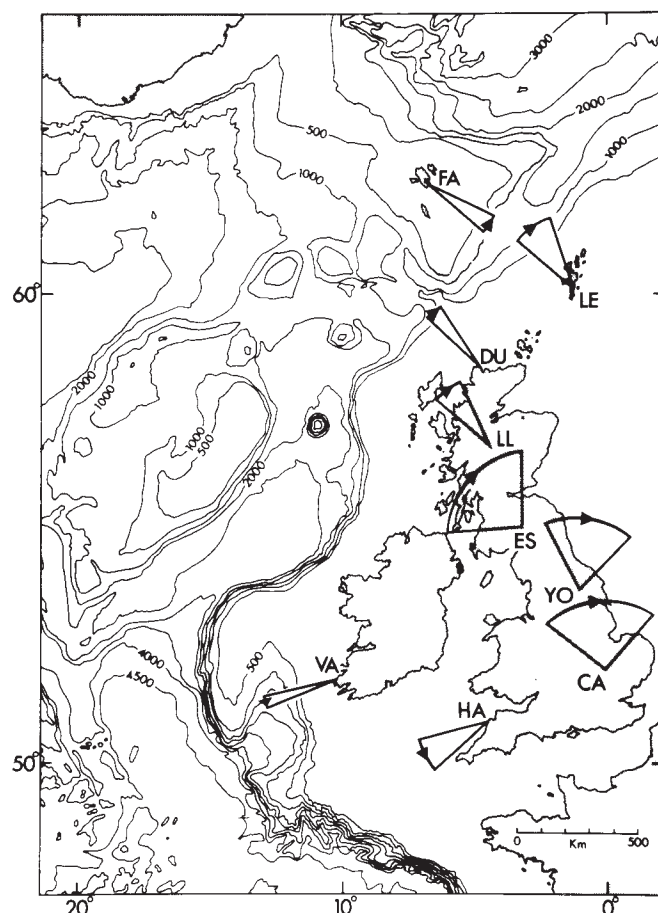


**Fig. 5.** Bathymetry of the west European continental margin contoured at an interval of 500 m. Also shown are the azimuths of the maximum response at 7200 and 900 s, at nine locations. The arrows denote the sense of rotation with decreasing period

the presence of both oceanic crust and continental fragments in the region (Laughton and Roberts, 1978). A relatively straightforward continental slope from deep ocean may only be defined to the SW of Britain, below a latitude of  $55^\circ$  N. In terms of the likely influence of induced currents in the deep ocean in the near-field (i.e.  $x < 500$  km), the three northern sites (DU, LE and FA) must be viewed as distinct from the two southern sites (VA and HA).

At the two southern sites, VA and HA, the frequency response is characterised by the occurrence of a maximum response in the period range 100–1000 s. In the vicinity of the maximum, the imaginary response displays a minimum, giving rise to a maximum response that is largely in-phase. For these two sites we may then define a long-period 'asymptotic' response curve for periods in excess of 1000 s. The site VA on the west coast of Ireland is the only site within 500 km of the deep ocean. The long-period response from this site may therefore be compared with the results obtained from the thin-sheet model for an ocean of depth 4 km, discussed previously. The comparison, in terms of  $G_R$  and  $G_I$ , is shown in Fig. 7 for model results obtained at a distance of  $x = 200$  km from the ocean edge. This distance roughly corresponds to the distance between the site and the shelf-sea margin. Given the simplicity of the model, a quantitative comparison is not warranted. However, the correct long-period asymptotic behaviour is clearly displayed by the observations. The level of corre-

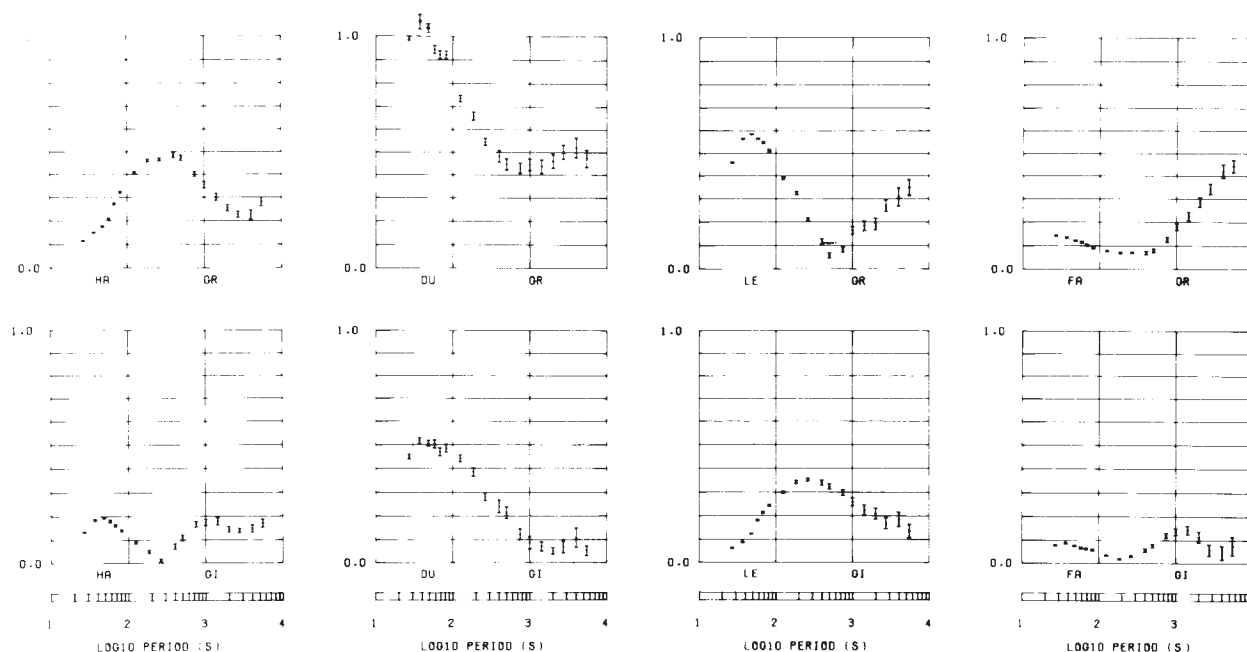


Fig. 6. Frequency response curves at four of the coastal sites shown in Fig. 5.  $G_R$ : magnitude of the real induction arrow.  $G_I$ : magnitude of the imaginary induction arrow

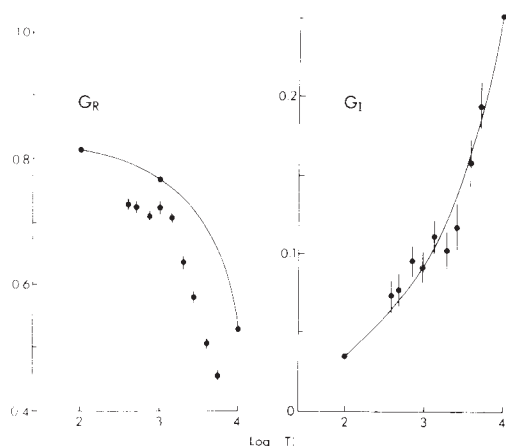


Fig. 7. Comparison of observed and calculated real ( $G_R$ ) and imaginary ( $G_I$ ) response magnitudes at VA. The solid line is calculated from a thin-sheet model of the deep ocean (4 km) at a distance of 200 km from the ocean edge

spondence shown in Fig. 7 is not displayed at any other of the coastal sites, as anticipated given the bathymetric information of Fig. 5.

Turning now to the response curves at the three northern coastal sites DU, LE and FA (Fig. 6), we observe very different and distinct frequency characteristics at each of the three locations. The only common feature appears to be a minimum in the  $G_R$  response in the period range 100–1000 s, at each of the three sites. The existence of a short-period (< 100 s) maximum in  $G_R$  may indicate the influence of an induction process taking place in the shallow shelf seas. However, the asymptotic behaviour of  $G_I$  does not generally exhibit the predicted behaviour. The very different frequency response curves at periods less than 1000 s observed on the two shelf-sea islands of Shetland (LE) and Faroe (FA) is worthy of note.

### The frequency characteristics at mainland sites

The single-site transfer functions within mainland Britain are far more numerous than at coastal sites. In order to examine spatially representative frequency characteristics it is necessary to subdivide the existing data set into regional data sets. Four representative regions have been chosen. The four regions cover that part of Britain lying between the Grampian Highlands of Scotland and northern England. To display each regional data set the simplest method of presentation is used, i.e. an overlay plot of individual results within each region. When the transfer function estimates are well-resolved this simple approach is adequate. The four parameters used for display are the magnitude and azimuth of the two induction arrows.

The four representative regions (R1–R4), together with the individual site locations, are shown in Fig. 8. It is worth noting that the regions cover two of the main structural elements of Caledonian Britain. The sites within region 1 (R1) lie within the Caledonian metamorphic foreland. The sites within the three regions to the south lie roughly within the Southern Uplands (R2), the Northumberland Basin (R3) and the Alston Block of northern England (R4). The combined results for each of the four regions are displayed in Fig. 9. The results are plotted on a common scale and define, quite clearly, the limiting bounds on the magnitude of the frequency response observed over a considerable area of northern Britain. The range of upper bounds in both real and imaginary magnitudes are lower by at least a factor of two when compared to the range of upper bounds observed at the coastal sites presented in Fig. 6.

Considering the complete frequency response curves for the four regions, it is apparent that the response characteristics of regions R2 and R3, the Southern Uplands and Northumberland Basin, exhibit common features. Regions R1 and R4 exhibit separate and distinct response characteristics to R2, R3. Within all four regions we observe an important frequency characteristic in the two azimuthal re-

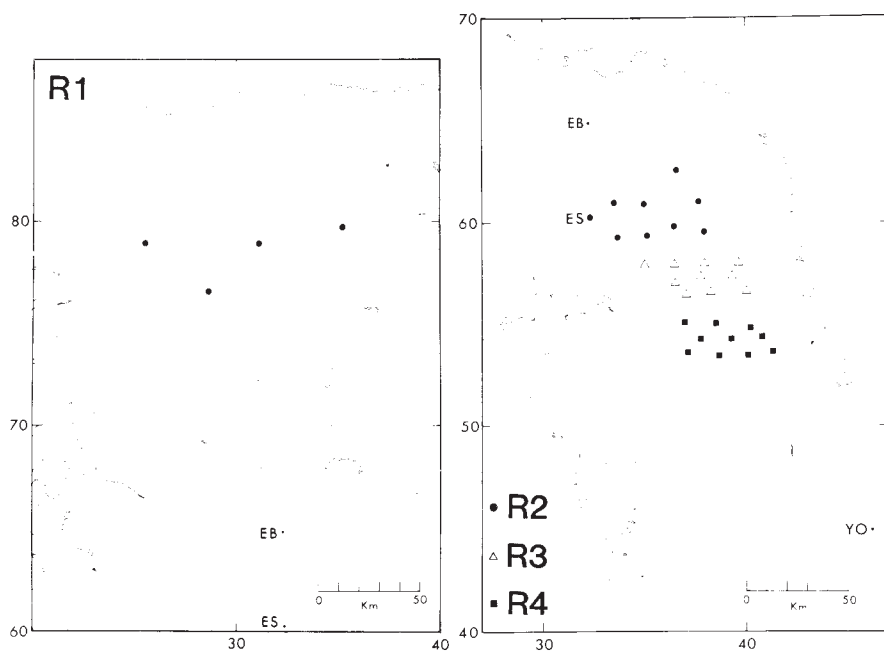


**Fig. 8.** Site locations within the four regions (R1–R4) referred to in the text. Coordinate numbers refer to the National Grid (ten units = 100 km). Geographical coordinates are provided in Fig. 5

sponses. With decreasing period, below 1000 s, the azimuths rotate to define local, rather than regional, strike directions. The rotation to predominantly local azimuths, increases with decreasing period. The obvious exception to this is  $\theta_R$  in region 4 (R4) which is highly constrained. Region 1 is characterised from all other regions by its long-period ( $>1000$  s) imaginary response  $G_I$ ,  $\theta_I$ . At periods in excess of 1000 s the imaginary azimuth appears consistent at the four widely separated sites. Again it is the imaginary response  $G_I$ ,  $\theta_I$  that characterises the frequency response in regions 2 and 3. In these two regions both the magnitude and azimuth of the imaginary response appear to be consistently constrained in the period range 100–1000 s. The response in region 4 is characterised from the above three regions by both the real and imaginary parts of the response. The upper and lower bounding values in the magnitude of  $G_R$  is quite apparent, as is the constraint on  $\theta_R$  at periods less than 1000 s. A second characteristic feature of region 4 is the short-period (60 s) maximum observed in the imaginary component. The induced current systems responsible for the anomalous vertical field characteristics observed in region 4 are considered by Beamish and Banks (1983) and Banks and Beamish (1984).

Clearly the rotation patterns from the NW to the NE quadrant, observed across regions 1 and 4 at periods in excess of 1000 s, confirm the large-scale effect of thin-sheet currents in the deep ocean and shelf seas noted previously. The lack of such a consistent rotation in regions 2 and 3 is likely to be due to the degree of attenuation experienced by the anomalous vertical field across these two regions. With the exception of region 4, which is in the near-field of regional east-west current flow, the rotation to local azimuths with decreasing period below 1000 s is clearly observed. Broadly, the results presented support the hypothesis proposed by Banks and Beamish (1984) that the anomalous vertical field at mainland sites responds principally to local geological structure only at periods less than 200 s.

#### The frequency characteristics considered in detail

The frequency characteristics observed in Fig. 9 define a set of regionally representative anomalous vertical-field estimates, presented in terms of induction arrows. In order to consider the characteristics in more detail we next reconsider the general frequency behaviour obtained previously from the simple 2-dimensional model. For the isolated conducting anomaly of Fig. 3, the existence of a characteristic period  $T_0$  was observed. At this period, a maximum anomalous vertical field is observed. Across such a period, the imaginary response together with the phase of the vertical field pass through zero and the azimuth difference ( $\theta_R - \theta_I$ ) changes by  $180^\circ$ . As noted previously, such 2-dimensional behaviour is most readily assessed using the magnitudes of the induction arrows together with the azimuth difference ( $\theta_R - \theta_I$ ) and the phase of the maximum response. Obviously,  $(\theta_R - \theta_I) = 0$  defines parallel induction arrows while  $(\theta_R - \theta_I) = 180^\circ$  defines antiparallel induction arrows. This method of presentation is displayed for a selection of four locations in Fig. 10a–d. The results for each of the four sites are now discussed in turn.

Figure 10a shows the frequency characteristics at York (YO, Fig. 5) near the eastern coast of England. The real magnitude ( $G_R$ ) exhibits two maxima with associated non-zero minima in the imaginary magnitude ( $G_I$ ). The lack of true zeros in  $G_I$  implies a departure from near-field 2-dimensionality. If we define two characteristic periods ( $T_0$ ) at the position of the above maxima, we observe that the phase passes through zero from positive values for  $T > T_0$  to negative values for  $T < T_0$ , as the model predicts. The behaviour of the azimuth difference, however, displays a smooth rotation through a large azimuth with frequency again indicating the absence of strong near-field 2-dimensionality.

The frequency characteristics observed in Fig. 10b at the coastal site of Hartland (HA, Fig. 5) are simpler to

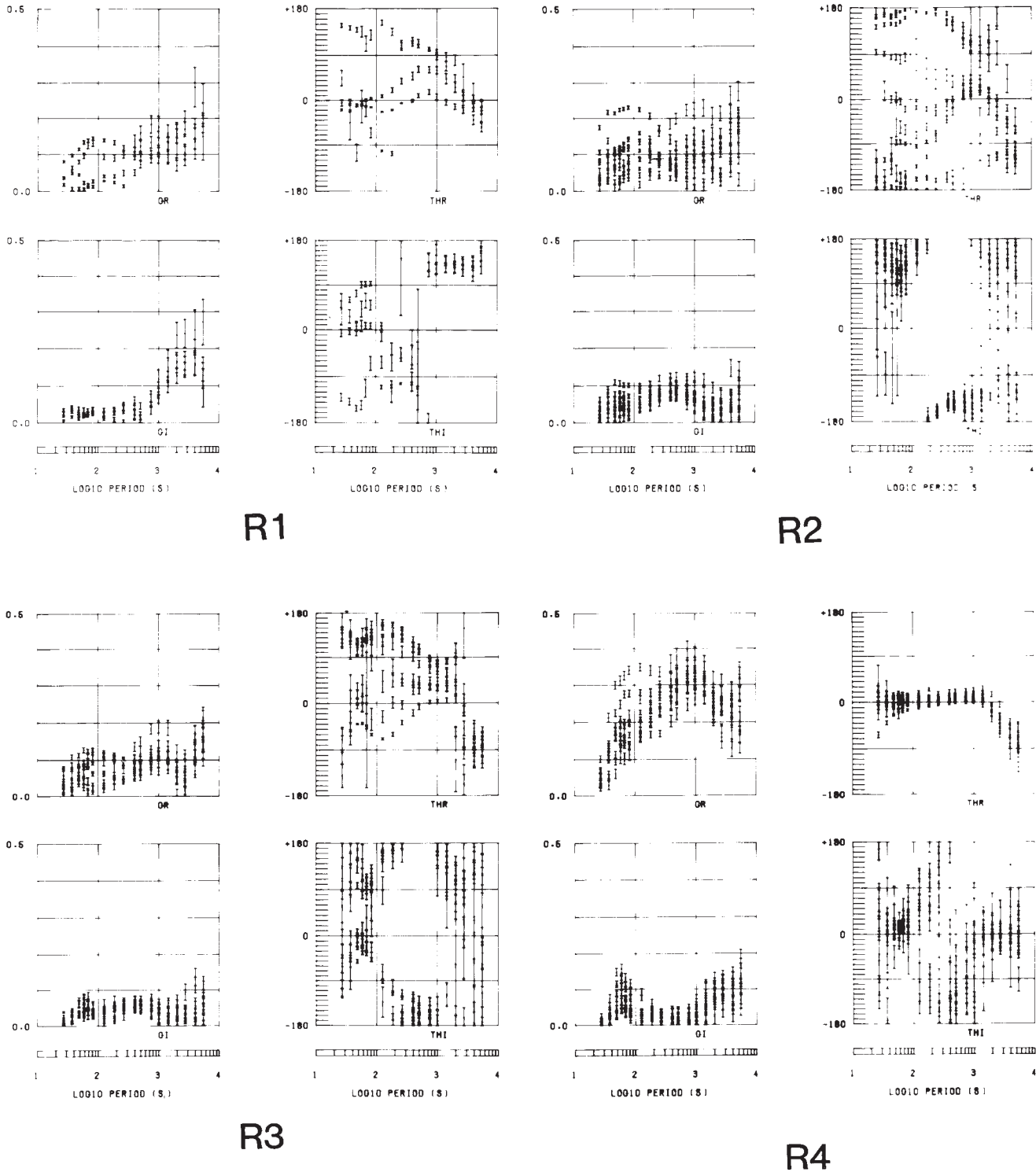


**Fig. 9.** Frequency response curves for the four regions R1–R4. Induction-arrow results overlaid.  $G_R$ ,  $G_I$ : induction-arrow magnitudes.  $THR$ ,  $THI$ : induction-arrow azimuths. (R1) 4 sites R1. (R2) 9 sites R2. (R4) 10 sites R3. (R3) 10 sites R4

interpret in that the location is truly coastal. A single maximum exists in the real magnitude with a corresponding true zero in the imaginary response. At periods just in excess of the characteristic period  $T_0$ , the phase is positive and  $(\theta_R - \theta_I)$  is zero. At periods slightly less than  $T_0$ , the phase is negative and the azimuth difference approaches  $-180^\circ$ . Thus, at periods close to  $T_0$ , the characteristic behaviour of a simple 2-dimensional conducting anomaly is observed.

At periods removed from  $T_0$ , the response departs from such simple behaviour which is not surprising given the complexity of the 'offshore conductor'.

The second two examples are taken from mainland locations and involve quite distinct 2-dimensional near-field effects. Figure 10c shows the frequency characteristics observed at Earlyburn (EB, Fig. 8) located in the vicinity of a major crustal Caledonian feature, the Southern Uplands



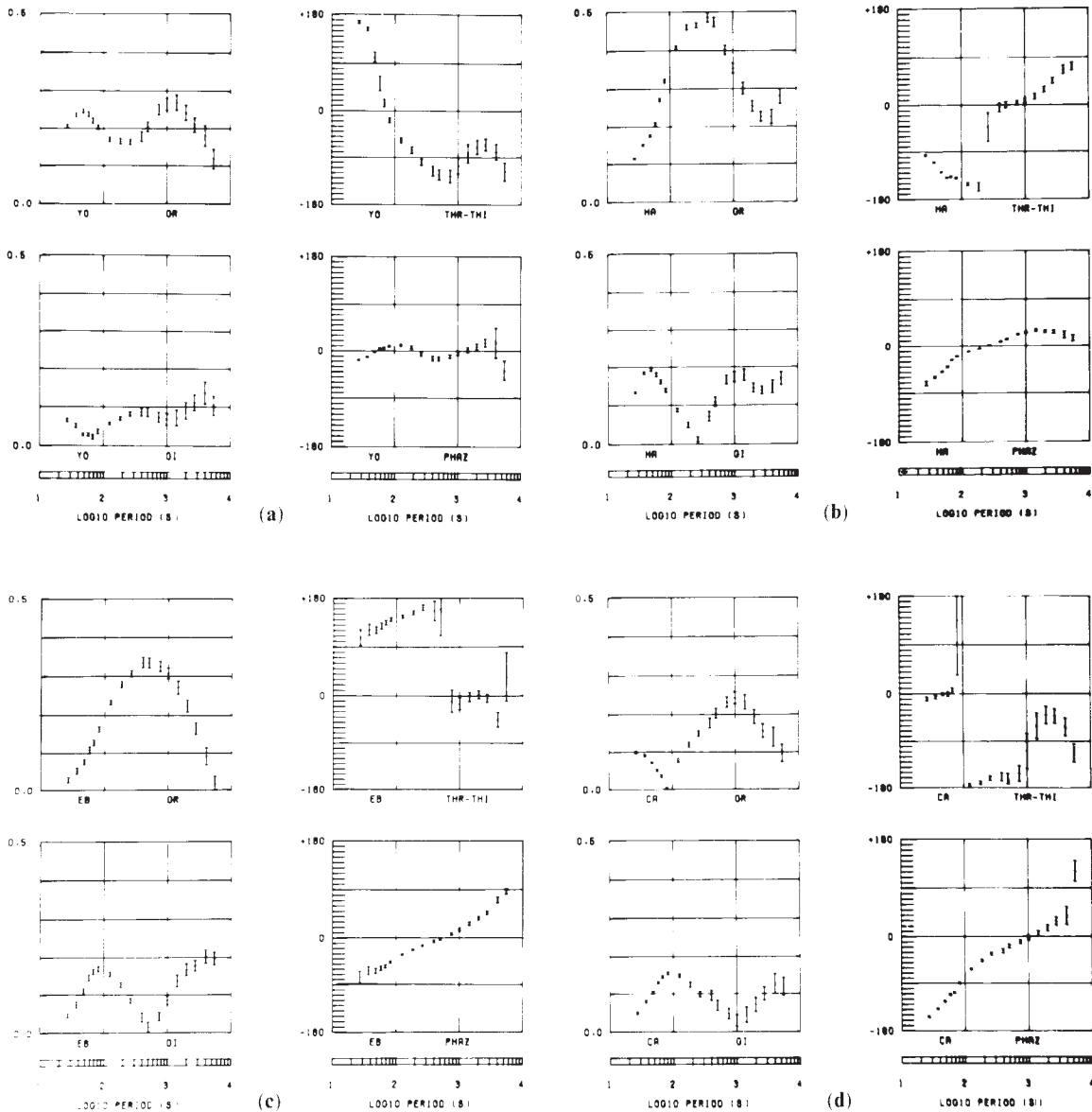


Fig. 10a–d. Frequency response curves at four locations.  $G_R, G_I$ : induction-arrow magnitudes.  $THR-THI$ : azimuth difference between real ( $G_R$ ) and imaginary ( $G_I$ ) induction arrows.  $PHAZ$ : phase of the maximum response. **a** Site YO. **b** Site HA. **c** Site EB. **d** Site CA

Fault. The distinct maximum observed is, in fact, the largest mainland response observed in the current data set. The features observed in all the parameters closely resemble the 2-dimensional effects of a single isolated conducting anomaly in the near-field. The 2-dimensional condition on the azimuth difference appears more consistent at longer rather than shorter periods.

Figure 10d shows the frequency characteristics observed at Cambridge (CA, Fig. 5). The long-period maximum at 1000 s owes its existence to off-shore induced currents as can be seen by comparing the response parameters observed in Fig. 10a and d and by noting the previously defined rotational properties at these sites at long periods. The interesting feature of Fig. 10d is the short-period maximum observed in the imaginary component and associated true zero in the real component. If we define a characteristic period  $T_0$ , at this maximum in  $G_I$ , we note that the phase passes through  $-90^\circ$  and the azimuth difference transfers from  $-180^\circ$  to  $0^\circ$  with decreasing period. Such behaviour conforms to that predicted for an isolated 2-dimensional

resistive anomaly observed in the near-field. The short-period behaviour observed at this site is unique among the current data set.

## Discussion

Following from the above work, it seems clear that in addition to providing information on the mechanisms of local and regional induction, the existence of a characteristic period observed within the broad-band frequency response curves goes some way to identifying the characteristic anomalous vertical field observed at a particular location. The use of the parameter pair consisting of phase and azimuth difference has been shown to be particularly effective in this regard. The existence of near- and far-field effects together with their interaction as a function of frequency will generally distort any simple concept of isolated 2-dimensionality. Despite the likely influence of such real Earth complexity, three of the frequency response curves presented in Fig. 10 display an adequate correspondence to

the behaviour anticipated from a single, isolated 2-dimensional anomaly. When such effects are observed it would be useful to establish some general relationships between the characteristic period observed and the anomaly from which they derive.

A large amount of Soviet work concerning the behaviour of anomalous magnetic field characteristics due to simple 2-dimensional structures is summarised by Rokityansky (1982). The type of models considered are insertion and graben surface structures together with immersed (i.e. buried) elliptical cylinders, the frequency response curves being calculated using analytical methods. It is clearly difficult, given the non-linearity of the problem, to obtain general results from even simple models. However, given the large number of models considered, Rokityansky (1982) considers general interpretational methods which may be applied in given situations. In particular, various estimation techniques to obtain the longitudinal conductivity ( $G = a \cdot b \cdot \sigma$  mho·m), defined by the cross-sectional area ( $a \cdot b$ ) of an anomalous body, are considered. For observations at a point at which the frequency response characteristics have been used to obtain the characteristic period  $T_0$ , Rokityansky (1982, eq. 6.63) suggests the empirical relationship

$$G = 5 \times 10^4 (T_0)^{1.2} \quad (4)$$

may be used to estimate longitudinal conductivity. The above relationship is the most probable result with maximum discrepancies occurring at a period of 400 s. For buried anomalies and structure with finite horizontal dimensions, the estimate obtained from the above will be an underestimate. From the strongly 2-dimensional frequency characteristics observed at EB (Fig. 10c),  $T_0$  is estimated as 700 s. Using the above,  $G$  is estimated as 129.74 mho·m. If we take the dimensional parameters for the Southern Uplands anomaly to be  $a = 10$  km and  $b = 100$  km, we obtain an estimate of the anomalous conductivity of 0.13 mho/m which is not unrealistic (Beamish, submitted for publication). When a characteristic period ( $T_0$ ) is observed at a coastal site, Rokityansky (1982, eq. 7.1) suggests an empirical formula relates  $T_0$  to the sea depth ( $h$ ):

$$T_0 = 250 \cdot (h)^{1.7} \quad (5)$$

with  $T_0$  in seconds and  $h$  in km. The characteristic period observed at the coastal site of HA (Fig. 10b) is estimated to be 200 s. Using the above relationship, the sea depth  $h$  is estimated to lie between 700 and 800 m. Such an estimate, bounded by the actual depths of shelf sea and deep ocean, seems reasonable. Since most of the published work concerns conductive (cf. resistive) anomalies, the characteristic short-period in-quadrature anomaly observed at CA (Fig. 10d) remains, for the present, an intriguing result.

**Acknowledgements.** I would like to thank Doug Quinney for providing the solutions for the thin-sheet ocean model used in this study. This paper is published with the approval of the Director, British Geological Survey (NERC).

## References

- Banks, R.J.: Data processing and interpretation in geomagnetic deep sounding. *Phys. Earth Planet. Inter.* **7**, 339–348, 1973  
 Banks, R.J., Beamish, D.: Local and regional induction in the British Isles. *Geophys. J.R. Astron. Soc.* **79**, 539–553, 1984  
 Banks, R.J., Ottey, P.: Geomagnetic deep sounding in and around the Kenya rift valley. *Geophys. J.R. Astron. Soc.* **36**, 321–335, 1974

- Beamish, D.: Deep crustal geoelectric structure under the North-umberland Basin. *Geophys. J.R. Astron. Soc.*, submitted, 1985  
 Beamish, D., Banks, R.J.: Geomagnetic variation anomalies in northern England: processing and presentation of data from a non-simultaneous array. *Geophys. J.R. Astron. Soc.* **75**, 513–539, 1983  
 Brewitt-Taylor, C.R., Weaver, J.T.: On the finite difference solution of two-dimensional induction problems. *Geophys. J.R. Astron. Soc.* **47**, 375–396, 1976  
 Dosso, H.W., Nienaber, W., Hutton, V.R.S.: An analogue model study of electromagnetic induction in the British Isles Region. *Phys. Earth Planet. Inter.* **22**, 68–85, 1980  
 Edwards, R.N., Law, L.K., White, A.: Geomagnetic variations in the British Isles and their relationship to electrical currents in the ocean and shallow seas. *Phil. Trans. R. Soc. Lond.* **A270**, 289–323, 1971  
 Fischer, G.: Electromagnetic induction effects at an ocean. *Proc. IEEE*, **67**, 1050–1060, 1979  
 Hewson-Browne, R.C., Kendall, P.C.: Magnetotelluric modelling and inversion in three-dimensions. *Acta Geodaet., Geophys. et Montanist.* **11**, 427–446, 1976  
 Hutton, V.R.S., Jones, A.G.: Magnetovariational and magnetotelluric investigations in S. Scotland. *Adv. Earth Planet. Sci.* **9**, 141–150, 1980  
 Jones, F.W.: Induction in laterally non-uniform conductors: theory and numerical models. *Phys. Earth Planet. Inter.* **7**, 282–293, 1973  
 Kaufman, A.A., Keller, G.V.: The magnetotelluric sounding method. *Methods in geochemistry and geophysics*, **15**, Amsterdam-Oxford-New York: Elsevier 1981  
 Kirkwood, S.C., Hutton, V.R.S., Sik, J.: A geomagnetic study of the Great Glen Fault. *Geophys. J.R. Astron. Soc.* **66**, 481–490, 1981  
 Laughton, A.S., Roberts, D.G.: Morphology of the continental margin. *Phil. Trans. R. Soc. Lond.* **A290**, 75–85, 1978  
 Lilley, F.E.M., Arora, B.R.: The sign convention for quadrature Parkinson arrows in geomagnetic induction studies. *Rev. Geophys. Space Phys.* **20**, 513–518, 1982  
 Parkinson, W.D.: The influence of continents and oceans on geomagnetic variations. *Geophys. J.R. Astron. Soc.* **6**, 441–449, 1962  
 Parkinson, W.D., Jones, F.W.: The geomagnetic coast effect. *Rev. Geophys. Space Phys.* **17**, 1999–2015, 1979  
 Pascoc, L.J., Jones, F.W.: Boundary conditions and calculations of surface values for the general two-dimensional electromagnetic induction problem. *Geophys. J.R. Astron. Soc.* **27**, 179–193, 1972  
 Quinney, D.A.: A note on computing coastal edge corrections for induced oceanic electric fields. *Geophys. J.R. Astron. Soc.* **56**, 119–126, 1979  
 Roden, R.B.: The effect of an ocean on magnetic diurnal variations. *Geophys. J.R. Astron. Soc.* **8**, 375–388, 1964  
 Rokityansky, I.I.: The interpretation of anomalous fields by using their frequency characteristics. *Phys. Earth Planet. Inter.* **10**, 271–281, 1975  
 Rokityansky, I.I.: Geoelectromagnetic investigation of the Earth's crust and mantle. Berlin-Heidelberg-New York: Springer-Verlag 1982  
 Schmucker, U.: Anomalies of geomagnetic variations in the southwestern United States. *Bull. Scripps Inst. Oceanogr., Monograph*, **13**, 1970  
 Schmucker, U.: Interpretation of induction anomalies above non-uniform surface layers. *Geophysics* **36**, 156–165, 1971  
 Sik, J.M., Hutton, V.R.S., Dawes, G.J.K., Kirkwood, S.C.: A geomagnetic variation study of Scotland. *Geophys. J.R. Astron. Soc.* **66**, 491–512, 1981  
 Weaver, J.T.: Electromagnetic induction in thin sheet conductivity anomalies at the surface of the Earth. *Proc. IEEE*, **67**, 1044–1050, 1979

Received March 1, 1985; Revised June 10, 1985

Accepted June 10, 1985